OPERATING CHARACTERISTICS OF A TWO-CAVITY X-BAND GYROKLYSTRON EXPERIMENT*

W. Lawson, J. Calame, D. Welsh, M.E. Read†, B. Hogan, M. Naiman,
P.E. Latham, M. Skopec, C.D. Striffler, M. Reiser, and V.L. Granatstein

Laboratory for Plasma Research
University of Maryland, College Park, MD 20742 USA

Abstract

At the University of Maryland we have designed and are operating a high power two-cavity TE_{01} gyroklystron in the 9.7–10.0 GHz range. The target beam power is derived from a 500 kV beam with a current ranging from 120–240 A in 1 μs pulses. The target microwave parameters for this tube include a power level of 15–30 MW with a gain of 25-30 dB. In this paper we summarize the initial characterization of the electron gun performance and detail preliminary tube stability and microwave amplification experiments.

Introduction

At the University of Maryland we are evaluating the suitability of gyroklystron amplifiers as RF power sources for linear colliders. The initial sequence of experiments involves characterizing a two cavity system to address questions of tube stability and amplifier efficiency. We have completed investigations of our first three configurations and are currently examining our fourth. A schematic of the major subsystems of the two-cavity gyroklystron[1] is shown in Fig. 1. A line-type modulator supplies the main voltage pulse and an intermediate voltage to a double anode Magnetron Injection Gun (MIG).[2] The beam is adiabatically compressed in an increasing magnetic field as it passes from the cathode (0.047 T) to the circuit (0.565 T). At a current of 160 A, the beam theoretically achieves a perpendicular-to-parallel velocity ratio of $\alpha = 1.5$ with an axial velocity spread of 7%. The beam's phase-space distribution is modulated in the first cavity by a signal from a 100 kW, 2 μs magnetron. Energy is extracted axially through a coupling aperture in the second cavity and travels through two non-linear tapers and the beam dump to a half-wavelength output window.

*Work supported by the U.S. Department of Energy.
†Physical Sciences, Inc., Alexandria, VA

Beam Characterization

Our electron gun is the first thermionic MIG to operate at 500 kV with a cathode loading of 30-60% of the predicted space-charge limit. While the steady-state simulations predict a high quality beam, various approximations involving self-fields are questionable and electrostatic instabilities are not addressed. Consequently, we constructed a beam diagnostic chamber in an attempt to measure several key parameters. In the beam quality experiment, the chamber replaced the microwave circuit in the overall configuration. Air core Rogowski coils at the entrance and exit measured beam current and interception. Capacitive probes measured line charge density, which together with the current yielded the average axial velocity. For small velocity spreads, the beam voltage could then be used to obtain the average α. The capacitive probes were split into four sectors to provide alignment information. A diamagnetic loop signal could be unfolded to indicate average transverse energy which was used as a check on α.

A comparison of theoretical and experimental space-charge limiting current is given in Table 1. Numerical simulations converged poorly below 250 kV due to non-laminar flow and experimental values above 350 kV could not be obtained due to modulator impedance limitations. The agreement is impressive, especially since the simulations predict a limit significantly exceeding idealized analytic estimates. A typical comparison between simulated and measured values of average α is given in Table 2. The agreement is quite good for higher currents. At low currents a low signal-to-noise ratio yields large error bounds. Furthermore, the velocity spread is quite large and the numerical assumption of uniform cathode loading is poor. An unexpected result, obtained by examining the time dependence of the probe signals, is that the average α is approximately 10% larger at the beginning of the pulse.

Table 1: Comparison of experimental and numerical space-charge limiting currents.

Voltage (kV)	Experimental Current (A)	Theoretical Current (A)
200	84	—
250	116	116
300	152	153
350	192	201
400	—	240
450	—	300
500	—	360

The diagnostic chamber was extremely susceptible to microwave oscillations. Below 175 kV, oscillations at $\sim$ 12.2 GHz occurred for $\alpha \approx 0.5$ (it was function of current). Above 175 kV, oscillations at $\sim$ 10.0 GHz disrupted the system at comparable velocity ratios. Attempts to avoid these resonances by adjusting the circuit magnetic field were unsuccessful, so the parameter space available for study was quite limited.

Microwave Tube Characterization

A schematic of the first two-cavity circuit is shown in Fig. 2. Microwaves are injected through a slit in the sidewall of the first cavity. The coupling loss was about 3 dB. The required input cavity Q (170) was obtained by placing carbon-impregnated ceramic rings on the side walls. Computer simulations[1] indicated that "whole tube" modes existing between the two cavities would disrupt amplifier operation. An attempt to stabilize these oscillations was made by constructing the drift tube with alternating rings of copper and silicon-carbide impregnated magnesia. The output cavity frequency and Q were 9.85 GHz and 175, respectively.

The main microwave diagnostic for the initial experiment was an anechoic chamber after the output window. Calibrated crystal detectors gave power estimates and an HP8566B spectrum analyzer gave frequency information. Positioning of the horn gave some mode information. Microwaves could also be sampled in the input cavity via the coupling slot and through a J-band horn looking at the back of the electron gun. Combined with local gas pressure measurements, the relative origin of spurious oscillations could be determined.

Tube operation was hampered by four types of microwave oscillations. Many modes existed in the output waveguide in regions where the output window is a good reflector. These modes are often eliminated by amplifier operation and are of little concern. Near the operating frequency of 9.85 GHz, there is a predominantly TE_{12} mode operating near cutoff in the output waveguide section between the second cavity and the first non-linear uptaper. This mode interferes with amplifier operation, but can be eliminated by slightly tapering the waveguide radius in that region. The third type of mode is the "whole tube" mode. These occurred at several frequencies with a particularly disruptive one slightly above 9 GHz. These oscillations were of concern because they existed at current levels significantly below theoretical start-oscillation predictions. The final mode class involved oscillations in the beam tunnel downtaper before the input cavity. The oscillations depended on beam voltage and current and circuit magnetic field, but would always appear when the velocity ratio exceeded ≈ 0.6. The modes tended to severely disrupt the beam and occurred in two bands: 7.0 – 7.5 GHz and 8.1 – 8.4 GHz (also $m = 1$ modes). The downtaper was loaded with lossy absorbers, but there was an all metal region between a gate valve and the taper which is susceptible to oscillations.

Table 2: Comparison of experimental and numerical average velocity ratios for a 150 kV beam.

Beam Current (A)	Experimental α	Theoretical α
7	0.98	0.38
12	0.58	—
22	0.32	0.33
37	0.25	—
44	0.19	0.22

A stable region for amplifier experiments was found at 80% of the nominal magnetic field at a beam voltage of 175 kV and a current of 55 A. Numerical simulations estimate the velocity ratio to be $\alpha \approx 0.45$ and the axial velocity spread to be about 4%. Our computer simulations of amplifier operation indicated that the gain would be about 0 dB under these restricted beam parameters. The experiment confirmed this prediction and output power was thus limited by the input source. Typical input and output crystal detector responses are shown in Fig. 3. The lower trace is the output signal and its reduced width corresponds to the duration of the voltage pulse.

At the completion of the initial experiment, the

tube was disassembled and the downtaper and drift tubes were cold-tested. The basic measurement involved transmission of the TE_{11} mode through these regions. It was found that while the drift tube was quite lossy at the design frequency, there were two broad regions in X-band alone where the ceramic rings exhibited virtually no loss. The downtaper attenuation varied from a high of 9.5 dB at 7.5 GHz to a low of 4.0 dB at 10.3 GHz. We believe that these low attenuations and the problems that reflections at the gate valve could introduce account for the more serious of the spurious oscillations.

For our second and third tubes, we made two major modifications to the two cavity experiment. First, the drift tube ceramics were replaced with silicon-carbide impregnated beryllia which had been arranged in a configuration so that the single-pass attenuation was always greater than 10 dB for the TE_{11} mode. Second, a new, longer downtaper was constructed. Its loss exceeded 20 dB from 7 to 8 GHz and was nowhere less than 11 dB through X-band. Furthermore, it covered the gate valve opening, thereby removing problems from reflections. These changes eliminated the troublesome 9 GHz whole tube mode and drastically reduced the effect of the beam tunnel modes. The enhanced stability resulting from the modifications allowed amplification studies up to 350 kV. Output powers in excess of 1.5 MW were achieved at 300 kV and $\approx$ 90 A. The optimum magnetic field and input frequency were 0.452 T and 9.866 Ghz, respectively. The gain was approximately 15 dB and the efficiency was roughly 5%. Operation was limited by the TE_{12} mode near 9.85 GHz and the remaining beam tunnel modes.

The fourth tube has a 2° taper of the output waveguide radius after the output cavity. This taper has eliminated the TE_{12} mode and has reduced the effect of several others. We are currently examining amplifier operation.

References

1. Lawson, W., et al., 1988 IEDM Tech. Digest, p. 162.

2. Lawson, W., et al., Int. J. Electron. 61, 969 (1986).

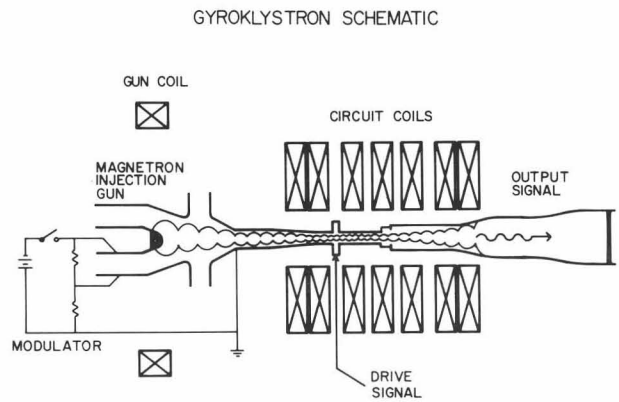

Figure 1: A simplified schematic of the two-cavity gyroklystron experiment.

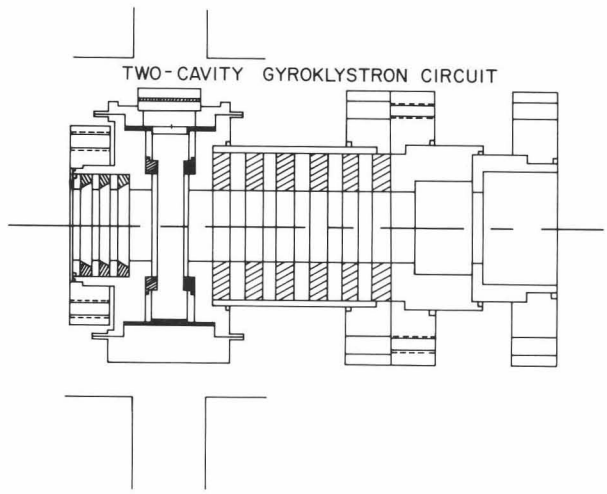

Figure 2: The initial two-cavity circuit.

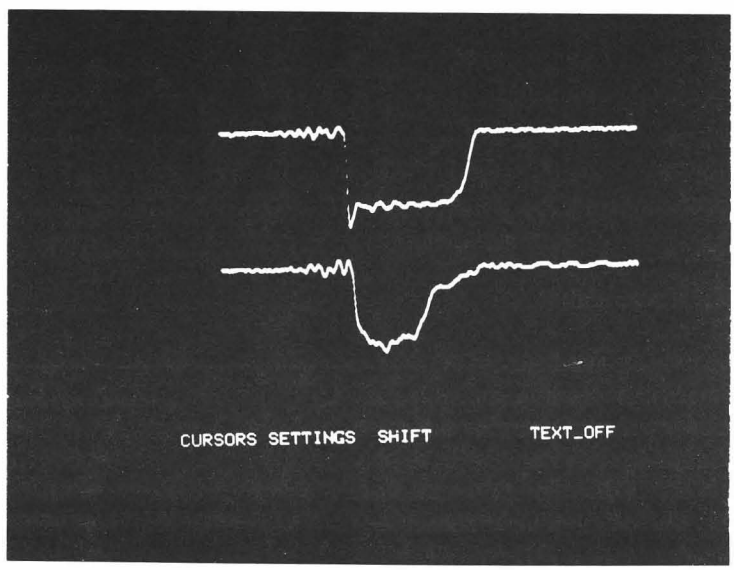

Figure 3: Crystal detector response of typical input and output microwave pulses. Lower pulse duration is $\sim 1\mu$s.